Lecture Notes of TICMI
Vol. 22, 2021, 31–46

Tension Failure Assessment of Composite Bolted Joints by Analytical Means

Minh Nguyen-Hoang*[a] and Wilfried Becker[a]

[a] *Institute of Structural Mechanics, Technical University of Darmstadt, Franziska-Braun-Straße 7, 64287 Darmstadt, Germany*

Many safety-relevant composite laminate parts in air- and spacecraft are connected by bolted joints. To ensure a safe and lightweight optimal design, precise structural analysis tools are crucial. Based on analytical methods, this work provides an efficient assessment framework to determine sustainable stresses of finite dimensions composite bolted joints, for which net section failure mode is triggered. First, the stress field is determined using Airy stress functions. Finite dimensions are modelled using auxiliary functions based on a novel period arrangement technique. Then, a failure analysis is conducted by the nonlocal prediction concepts of Finite Fracture Mechanics and the Theory of Critical Distances. The hole size effect is modelled and the influence of finite-width on the stress concentrations as well as the failure load reduction in the context of the size effect is discussed.

Keywords: Bolted joints, Composite laminates, Stress analysis, Tension failure, Theory of Critical Distances, Finite Fracture Mechanics

1. Introduction

The connection of safety-critical parts in air- and spacecraft can be done by bolted joints, which is advantageous in terms of inexpensive manufacturing and the possibility to disassemble, for instance. However, holes must be placed in the structure. This reduces its cross-section causing stress concentrations and precise means for structural assessment are crucial to ensure a safe and lightweight optimal design. Of special interest are connections with composite laminates as plate material, which provide advantages in terms of high stiffness and strength values relative to the material density, for example. In regard to structural assessment, the following five bolted joints failure modes shall be taken into account [1]: net section, shear-out, bearing, cleavage and pull-through failure depicted in Fig. 1. Which of the five mode occurs is influenced by many parameters. To name a few, these comprise joint geometry, clamping pressure as well as the composite laminate's stacking sequence and fibre orientation if such a plate material is used. Corresponding tests have been conducted by [2, 3] and a review regarding the parameters' influence on the failure modes can be found in [4]. Further, a summary concerning the mechanical modelling including stress and failure analysis as well as experimental validation is given by [5]. In general, bolted joint connections should be dimensioned such that bearing failure is likely to be triggered as this mode involves a gradual and fail-safe failure

*Corresponding author. Email: nguyen-hoang@fsm.tu-darmstadt.de

ISSN: 1512-0511 print

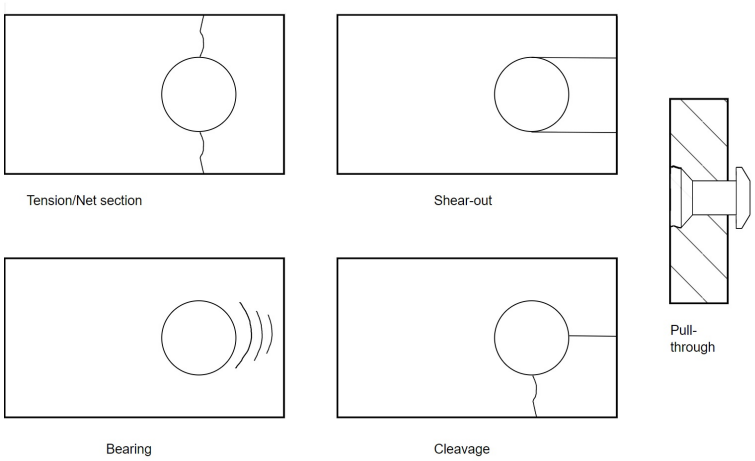

Figure 1. Bolted joint failure modes.

process. Corresponding experimental studies are, e.g., [6, 7]. For connections with a width-to-hole diameter ratio $w/d \leq 4$ (Fig. 2), net section failure is likely to occur [8] and the connection is instantaneously destroyed. This mode must be avoided in safety-critical parts under any circumstances and accurate means for stress and failure analysis are crucial for prevention. Focus of the present work is the development of such means using analytical methods, which are beneficial in terms of computational effort and should be documented in technical handbooks in the ideal case.

Generally, the structural assessment begins with a mechanical idealisation. Then, the corresponding stress field is determined, which is followed by a failure analysis, lastly. The load transfer of bolted joint connections is quite complex as it is characterised by a nonlinear contact problem and a three-dimensional stress state. Moreover, the sustainable load is affected by many parameters, e.g. width-to-hole diameter ratio w/d, hole size effect and lay-up [2, 3, 8]. Modelling all failure mechanism factors is expensive and hardly feasible when an analytical modelling approach shall be pursued. To reduce the complexity, let us idealise the bolted joint as a two-dimensional plane problem, which is still capable of capturing the main relevant effects of the load transfer and failure mechanism. This can be done for joints with an overall symmetrical setup with respect to the midplane so that no secondary bending effects exist. This is provided if the number of plates is uneven and the layup without bending extension coupling.

The stress analysis of this in-plane idealisation is often referred as pin-loaded hole or pinned hole. Its analytical stress field determination has been the subject of many researches with different level of complexity. A corresponding review is done by [1, 9], whereas [10] gives an overview about a variety of plate problems with holes and notches. In the context of the pinned-hole problem, the bolt contact is commonly idealised by radial tractions of sinusoidal shape along half of the hole boundary and friction is neglected [11]. This has been done also in the following publications. Regarding isotropic plates, [12] covers infinite dimensions and [13] finite width but infinite height both using the Airy stress function. The following works treat orthotropic plate material using complex potential method in the formalism by Lekhnitskii [14]: [15] deal with infinite and [16] finite plate dimensions. This is

achieved using correction factors, which heuristically scale the infinite domain solution such that its constant far-field stresses equilibrate the external load along the finite width. However, the stress-free conditions are violated at the edges parallel to the load direction. Hence, the results may be acceptable for connections with wider width-to-hole diameter ratios w/d containing slight finite-dimensions effects only. The stress calculus is implemented in an overall bolted joint assessment tool by [17]. Therein, the circumferential stresses reveal good agreement to a finite element analysis (FEA) for the layup $[0°/\pm 45°/90°]_s(50\%/40\%/10\%)$ and the rather large relative dimensions $w/d = 8,\ e/d = 9$. The latter geometry ratio represents the relative end distance (Fig. 2). By assessing the stress concentrations, it is further deduced that the analytical stresses are sufficiently accurate for the parameters $e/d = 9$ and $w/d > 4$. To lower the computational effort, the authors of [18] modify the heuristic solution by [16] using the first terms of the series for the stress field representation only. The derived concentrations are validated against the original calculus. However, there is no comparison of neither the stress concentrations nor their decay to that of the actual boundary value problem, which is vital to assess the method's capabilities when a failure analysis using nonlocal concepts shall be conducted. The following works implement finite dimensions by solving the actual boundary value problem. The authors of [19] approximate the rectangular plate geometry as an ellipse and good results in comparison to FEA in the circumferential stresses for $[\pm 45°]_s$ laminates and $w/d = 3$ as well as for $[0°/90°]_s$ laminates and $w/d = 5$ are achieved. Bending extension coupling is modelled by [20] showing good agreement to FEA for $w/d = \{15, 45\}$, which is a ratio leading to slight or even vanishing finite-width effects. The authors of [21] extend this method to multilayered composite bolted joints with interference-fit and thermal load. An approach continuously fulfilling the load transfer relevant stress boundary conditions is given by [22]. Therein, quasi-isotropic bolted joints are investigated using Airy stress functions. However, the stress boundary conditions along the straight edges perpendicular to the load direction are not covered and slight deviations in comparison to FEA arise. The present work shall cure this drawback by adapting the calculus of [23] for open holes, which is documented in [24]. Then, the derived stress field serves as input for the subsequent failure analysis conducted by nonlocal concepts.

The failure analysis for structures with brittle fracture can be conducted by means of local and nonlocal criteria. The former require to evaluate the stress concentration directly at the hole edge and has been used to assess many problems [25–28]. Contrary, the latter criteria require the stress evaluation at or averaged within a certain hole distance. Beneficial is the capability of capturing the size effect. Be referred to [29–34] for literature regarding this phenomenon. The Theory of Critical Distances [35–39] as well as the recent state of the art concept Finite Fracture Mechanics [40–42] are frequently used nonlocal criteria. Regarding bolted joints, the first criterion is applied by [22, 43] and the second by [22, 44]. In both, the failure concepts are validated against experimental test data published by [44]. In this work, based on an enhanced stress solution, both concepts are used to model the size effect. In this context, the finite-width influence on the failure load reduction for increasing defect sizes is investigated.

2. Stress field determination

In the following, a methodology to determine the stress field of the bolted joint with finite dimensions (Fig. 2) is developed. Therein, the quantity P_y denotes the external force per plate thickness, which is applied in the vertical direction. Furthermore, w is the plate width, e the plate end distance and d the hole diameter. The bolt contact is idealised by a sinusoidal radial traction distribution along the upper hole boundary. This study shall be dedicated to quasi-isotropic composite laminates and the Airy stress function is used to represent the stress field. Once the present approach has proven feasible, the more general case of orthotropic plate material may be treated. Note that the overall methodology would stay the same. Only complex potentials [14, 45] instead of Airy stress functions, then, are to be used.

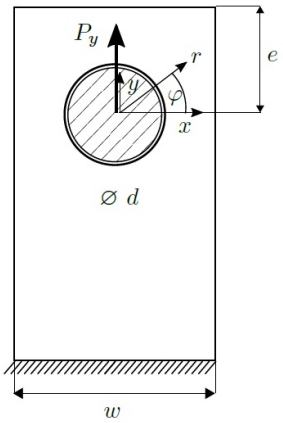

Figure 2. Bolted joint with finite dimensions.

2.1. *Airy stress function*

In the following, let us neglect any influence by clamping pressure. Then, a two-dimensional plane stress state is given and with linear elastic and isotropic material behaviour in addition, the governing equations for equilibrium, compatibility and Hooke's law can be ensured using one single differential equation. In doing so, use is made of the Airy stress function F, which requires to obey the biharmonic equation [46, 47]

$$\Delta\Delta F = 0 \qquad \text{with}$$

$$\Delta = \begin{cases} \dfrac{\partial^2 F}{\partial x^2} + \dfrac{\partial^2 F}{\partial y^2} & \text{in cartesian coordinates,} \\ \dfrac{\partial^2}{\partial r^2} + \dfrac{1}{r}\dfrac{\partial}{\partial r} + \dfrac{1}{r^2}\dfrac{\partial^2}{\partial \varphi^2} & \text{in polar coordinates.} \end{cases} \tag{1}$$

This is satisfied when using biharmonic functions [48]. The corresponding stress components can be derived using

$$\sigma_x = \frac{\partial^2 F}{\partial y^2}, \qquad \sigma_y = \frac{\partial^2 F}{\partial x^2}, \qquad \tau_{xy} = -\frac{\partial^2 F}{\partial x \partial y}, \tag{2}$$

$$\sigma_r = \frac{1}{r}\frac{\partial F}{\partial r} + \frac{1}{r^2}\frac{\partial^2 F}{\partial \varphi^2}, \qquad \sigma_\varphi = \frac{\partial^2 F}{\partial r^2}, \qquad \tau_{r\varphi} = -\frac{\partial}{\partial r}\left(\frac{1}{r}\frac{\partial F}{\partial \varphi}\right). \tag{3}$$

Task is now to determine the stress functions such that the stress boundary conditions of the bolted joint idealisation are fulfilled. By assuming no friction and

sinusoidal radial tractions [11], these read

$$\sigma_r(R,\varphi) = \begin{cases} -\dfrac{2}{\pi}\dfrac{P_y}{R}\sin\varphi & \text{for} \quad 0 \le \varphi \le \pi, \\ 0 & \text{for} \quad \pi \le \varphi \le 2\pi, \end{cases} \tag{4}$$

$$\tau_{r\varphi}(R,\varphi) = \quad 0 \qquad\qquad \text{for} \quad 0 \le \varphi \le 2\pi.$$

Furthermore, the given finite dimensions are taken into account by

$$\begin{gathered} \sigma_x(\pm w/2, y) = \tau_{xy}(\pm w/2, y) = 0, \\ \sigma_y(x, e) = \tau_{xy}(x, e) = 0. \end{gathered} \tag{5}$$

The overall calculus starts with determining the stress field of the infinite dimensions bolted joint. This requires to find a stress function satisfying the hole boundary conditions in Eq. (4) only. Then, auxiliary functions are developed and superimposed such that the boundary conditions in Eq. (5) are fulfilled in addition and finite dimensions are modelled.

2.2. *Infinite domain solution*

The radial tractions are applied along the upper half of the hole edge, whereas the remaining lower half remains unloaded. This can be analytically expressed using Fourier series expansion. Using the reference stress $\sigma_0 = P_y/d$ the hole boundary conditions then read

$$\begin{aligned} \sigma_r(R,\varphi)/\sigma_0 &= -\frac{2}{\pi}\sin\varphi \underbrace{-\frac{4}{\pi^2} - \sum_{n=1}^{N} \frac{4}{\pi^2}\frac{1+\cos 2n\pi}{1-4n^2}\cos 2n\varphi}_{\text{cosine Fourier series of } |-2/\pi \sin\varphi|}, \\ \tau_{r\varphi}(R,\varphi)/\sigma_0 &= 0. \end{aligned} \tag{6}$$

This stress distribution modelling the bolt load introduction (LI) is produced by the stress function

$$F^{\mathrm{LI}} = F^{\mathrm{LI},1} + F^{\mathrm{LI},2}. \tag{7}$$

Therein, the first term models a full sine and the second the cosine Fourier series part of the radial hole tractions. In particular

$$F^{\mathrm{LI},1} = \frac{R}{\pi}\left[r\varphi\cos\varphi + \frac{1}{2}(1-\nu)\, r \ln\frac{r}{R}\sin\varphi + \frac{1}{4}(1-\nu)\, R^2\frac{1}{r}\sin\varphi\right]\sigma_0, \tag{8}$$

$$F^{\mathrm{LI},2} = R^2\left[b_2 \ln\frac{r}{R} + \sum_{n=1}^{N}\left\{A_{2,n}\left(\frac{R}{r}\right)^{2n} + B_{2,n}\left(\frac{R}{r}\right)^{2n-2}\right\}\cos 2n\varphi\right]\sigma_0. \tag{9}$$

The corresponding stress components can be derived by Eq. (2), (3). Equating the coefficients of the radial hole tractions produced by the stress function $F^{\mathrm{LI},2}$ with the Fourier series expansion in Eq. (6) reveals

$$b_2 = \frac{f_{2,0}}{2}, \quad A_{2,n} = -\frac{2n-1}{2n+1} B_{2,n}, \quad B_{2,n} = \frac{1}{2} \frac{f_{2,2n}}{n(2n-1) - (n+1)(2n-1)},$$

$$f_{2,n} = \begin{cases} -\frac{4}{\pi^2} \frac{1+\cos n\pi}{1-n^2} & \text{for even } n, \\ 0 & \text{for odd } n. \end{cases} \tag{10}$$

Refer to [22–24] for further details.

2.3. *Finite domain solution*

To implement finite dimensions by satisfying the stress-free boundary conditions in Eq. (5) in addition, use is made of the following three types of auxiliary stress functions. The first function aims to eliminate nonzero shear tractions $\tau_{xy}(\pm w/2, y)$ as well as normal tractions $\sigma_y(x, e)$. These tractions show in load direction and their cancellation is crucial to equilibrate the external bolt force by the net section stresses alone (ref. Fig. 3 for illustration). The second function cancels nonzero normal tractions $\sigma_x(\pm w/2, y)$ acting perpendicularly to the load direction and lastly the third function cures violated hole boundary conditions. These may arise due to the other two correction stress functions. In general, each of them is dedicated to a certain set of stress boundary conditions and even may interfere with others. To fulfil each simultaneously nevertheless, the three different types of correction functions are applied iteratively until violations are negligibly small. The different auxiliary stress functions are now further specified.

2.3.1. Elimination of tractions in load direction

The first auxiliary stress function cancels the nonzero tractions $\tau_{xy}(\pm w/2, y)$ and $\sigma_y(x, e)$ of the infinite domain solution F^{LI}. These tractions show in load direction and are cancelled using auxiliary stress fields, which are created by taking the infinite domain solution and arranging it periodically as illustrated in Fig. 4. Along the finite boundaries, the stresses addressed have the same magnitude but a reversed sign enabling elimination. The position and orientation of each auxiliary stress function is determined by

$$F_{ij}^{\mathrm{LI}}(x, y) = \underbrace{(-1)^{i+1}}_{\substack{\text{Tension/} \\ \text{Compression}}} \cdot F^{\mathrm{LI}}\Big(\underbrace{(-1)^{i+1} x_j, (-1)^{i+1}}_{\text{load shifting along hole}} y_i \Big), \tag{11}$$

$$\text{with} \quad [x_j] = [x_1 \quad x_2 \quad x_3 \quad x_4 \quad ...] = [x \quad x-w \quad x+w \quad x-2w \quad ...], \tag{12}$$

$$[y_i] = [y_1 \quad y_2] = [y \quad y-2e]. \tag{13}$$

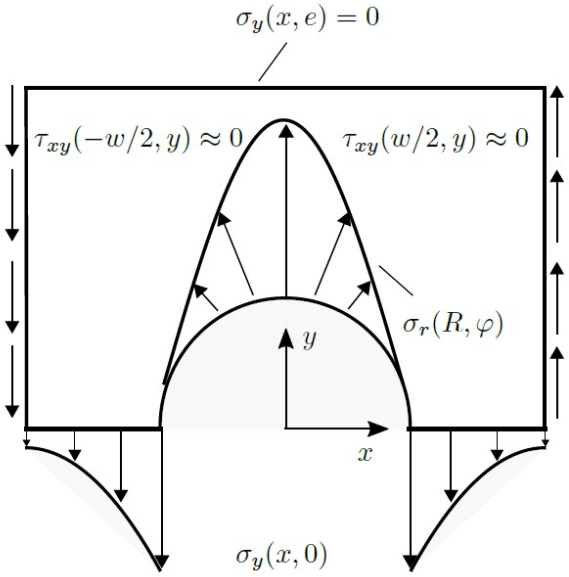

Figure 3. Free form body showing the stresses affecting the equilibrium in load/y-direction only. The shear tractions $\tau_{xy}(\pm w/2, y)$ need to be negligibly small such that the net section stresses $\sigma_y(x,0)$ transfer the whole bolt load alone.

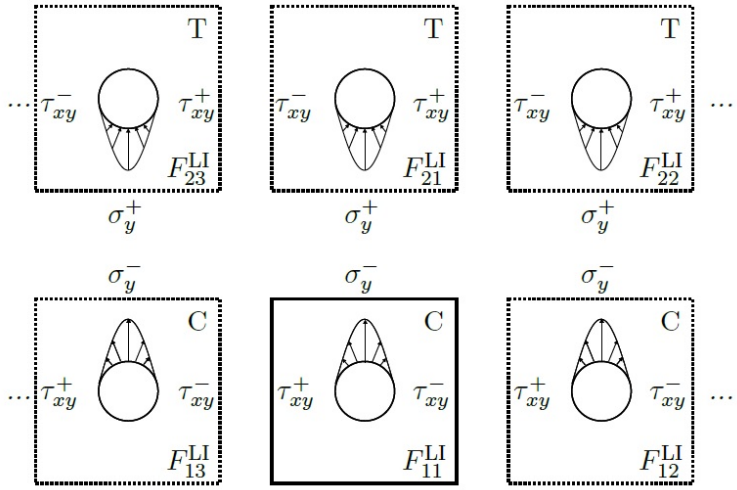

Figure 4. Virtual periodic auxiliary functions.$F^{\mathrm{LI}} = F_{11}^{\mathrm{LI}}$. C $\hat{=}$ Compression, T $\hat{=}$ Tension.

The periodic arrangement (PA) is implemented using the operator

$$\mathrm{PA}\left(F^{\mathrm{LI}}\right) = \sum_{i=1}^{n_y=2} \sum_{j=1}^{n_x} F_{ij}^{\mathrm{LI}}, \tag{14}$$

where n_y is the number of auxiliary stress functions aligned in vertical/y-direction and n_x that of the auxiliary stress functions in the horizontal/x-direction. The latter quantity is obtained by the demand of less than 0.5 % inaccuracy in the load transfer,

which is expressed by the condition

$$\psi_{\tau_{xy}^{\mathrm{LI}}} = \frac{2}{P_y} \left| \int_0^e \sum_{i=1}^{n_y=2} \sum_{j=1}^{n_{x,\min}} \tau_{xy,ij}^{\mathrm{LI}}(\pm w/2, y)\, \mathrm{d}y \right| \leq 0.5\ \%. \tag{15}$$

Refer to Fig. 3 for illustration how to derive this condition. Refer to [22–24] for further details concerning the overall stress calculus including the periodic arrangement concept for implementation of stress-free straight edges of finite domain problems.

2.3.2. Elimination of tractions perpendicular to the load direction

To cancel the nonzero stresses $\sigma_x(\pm w/2, y)$ perpendicular to the load direction along the vertical edges (VE), the correction stress function $F_k^{\mathrm{VE}\perp}$ is introduced. When investigating the periodic arrangement in Fig. 4 the superimposed stress field contains the antisymmetry axis $y = e$. In accordance to the nomenclature in [23, 24], let k be a placeholder for any stress field with this symmetry characteristics containing these deviating (dev) stress boundary conditions to cure. Then, the violations fulfil

$$\sigma_{x,k}^{\mathrm{dev}}(\pm w/2, y^*) = -\sigma_{x,k}^{\mathrm{dev}}(\pm w/2, -y^*) \qquad \text{with} \quad y^* = y - e, \tag{16}$$

and can be expanded using a Fourier series of the form

$$\begin{aligned} \sigma_{x,k}^{\mathrm{VE}\perp}(\pm w/2, y^*)/\sigma_0 &= \sum_{n_k=1}^{N_k} f_{k,n}^{\sigma_x} \sin \alpha_n\, y^* \quad \text{with} \\ \alpha_n = \frac{2n\pi}{l}, &\quad f_{k,n}^{\sigma_x} = \frac{2}{l} \int_0^{l_k} \sigma_{x,k}^{\mathrm{dev}}(\pm w/2, y^*) \sin \alpha_n\, y^*\, \mathrm{d}y^*. \end{aligned} \tag{17}$$

Therein, the Fourier wave length l should be chosen sufficiently long, e.g. $l = 40\, d$. The stress functions capable of modelling those Fourier series expansions in Eq. (17) are of the general form [46, 49]

$$\begin{aligned} F_k^{\mathrm{VE}\perp}/\sigma_0 &= \sum_{n=1}^{N_k} \phi_n(x)\, A_{k,n}^{\mathrm{VE}\perp} \sin \alpha_n\, y^* \quad \text{with} \\ \phi_n(x) &= C_1^{\phi_n} \cosh \alpha_n\, x + C_2^{\phi_n} \sinh \alpha_n\, x + C_3^{\phi_n} x \cosh \alpha_n\, x + C_4^{\phi_n} x \sinh \alpha_n\, x. \end{aligned} \tag{18}$$

Equating the coefficients of the stresses produced by $F_k^{\mathrm{VE}\perp}$ using Eq. (2) with those of the stress deviation's Fourier series representation in Eq. (17) and the requirement

of any shear tractions $\tau_{xy,k}^{\mathrm{VE}\perp}(\pm w/2, y) = 0$ by the correction stress function leads to

$$A_{k,n}^{\mathrm{VE}\perp} = -\frac{f_{k,n}^{\sigma_x}}{\alpha_n^2}, \tag{19}$$

$$C_1^{\phi_n} = \frac{2\sinh w/2\,\alpha_n + \alpha_n w\cosh w/2\,\alpha_n}{\sinh w\,\alpha_n + w\,\alpha_n}, \quad C_2^{\phi_n} = C_3^{\phi_n} = 0, \tag{20}$$

$$C_4^{\phi_n} = -\frac{2\,\alpha_n \sinh w/2\,\alpha_n}{\sinh w\,\alpha_n + w\,\alpha_n}. \tag{21}$$

2.3.3. Mitigation of violated hole boundary conditions

Be reminded that each of the correction stress functions addresses only a certain set of stress boundary conditions and may even interfere with another. By the first two correction stress functions introduced the sinusoidal bolt load introduction in Eq. (4) may be disturbed and a corresponding mitigation stress function is required. Let us expand the deviating hole boundary conditions (HBC) using the Fourier series

$$\sigma_{r,k}^{\mathrm{HBC}}(R,\varphi)/\sigma_0 = \frac{f_{k,0}^{\sigma_r}}{2} + \sum_{n=1}^{N^*} f_{k,n}^{\sigma_r}\cos n\varphi + \sum_{n=1}^{N^*} g_{k,n}^{\sigma_r}\sin n\varphi, \tag{22}$$

$$\tau_{r\varphi,k}^{\mathrm{HBC}}(R,\varphi)/\sigma_0 = \frac{f_{k,0}^{\tau_{r\varphi}}}{2} + \sum_{n=1}^{N^*} f_{k,n}^{\tau_{r\varphi}}\cos n\varphi + \sum_{n=1}^{N^*} g_{k,n}^{\tau_{r\varphi}}\sin n\varphi. \tag{23}$$

With the deviating hole tractions $\sigma_{rk}^{\mathrm{dev}}(R,\varphi)$ and $\tau_{r\varphi k}^{\mathrm{dev}}(R,\varphi)$ to be cancelled, the Fourier coefficients are

$$\begin{aligned}
f_{k,n}^{\sigma_r} &= \frac{1}{\pi}\frac{1}{\sigma_0}\int_0^{2\pi} \sigma_{rk}^{\mathrm{dev}}(R,\varphi)\cos n\varphi\,\mathrm{d}\varphi,\\
g_{k,n}^{\sigma_r} &= \frac{1}{\pi}\frac{1}{\sigma_0}\int_0^{2\pi} \sigma_{rk}^{\mathrm{dev}}(R,\varphi)\sin n\varphi\,\mathrm{d}\varphi,\\
f_{k,n}^{\tau_{r\varphi}} &= \frac{1}{\pi}\frac{1}{\sigma_0}\int_0^{2\pi} \tau_{r\varphi k}^{\mathrm{dev}}(R,\varphi)\cos n\varphi\,\mathrm{d}\varphi,\\
g_{k,n}^{\tau_{r\varphi}} &= \frac{1}{\pi}\frac{1}{\sigma_0}\int_0^{2\pi} \tau_{r\varphi k}^{\mathrm{dev}}(R,\varphi)\sin n\varphi\,\mathrm{d}\varphi.
\end{aligned} \tag{24}$$

Taking into account that the present bolted joint problem is symmetric to the y-axis, only the even coefficients $f_{k,n}^{\sigma_r}, g_{k,n}^{\tau_{r\varphi}}$ and the uneven coefficients $g_{k,n}^{\sigma_r}, f_{k,n}^{\tau_{r\varphi}}$ are nonzero.

Then, the stress function modelling the violated hole tractions has the general form

$$F_k^{\mathrm{HBC}} = R^2\Bigg[b_k^{\sigma_r}\ln\frac{r}{R} + c_k^{\sigma_r}\frac{r}{R}\,\varphi\cos\varphi + d_k^{\sigma_r}\frac{r}{R}\ln\frac{r}{R}\sin\varphi + d_k^{\tau_{r\varphi}}\frac{R}{r}\sin\varphi + \\ + \sum_{n=1}^{N}\left\{A_{k,n}\left(\frac{R}{r}\right)^{2n} + B_{k,n}\left(\frac{R}{r}\right)^{2n-2}\right\}\cos 2n\varphi \\ + \sum_{n=1}^{N}\left\{C_{k,n}\left(\frac{R}{r}\right)^{2n+1} + D_{k,n}\left(\frac{R}{r}\right)^{2n-1}\right\}\sin(2n+1)\,\varphi\Bigg]\,\sigma_0. \quad (25)$$

The corresponding coefficients are determined by ensuring single-valued displacements [12, 46] yielding

$$\frac{d_k^{\sigma_r}}{c_k^{\sigma_r}} = \frac{1}{2}(1-\nu), \quad (26)$$

and then deriving the hole tractions produced by F_k^{HBC} using Eq. (3) and equating them with the Fourier series expansion in Eq. (23). Eventually, we obtain

$$b_k^{\sigma_r} = \frac{1}{2}\,f_{k,0}^{\sigma_r}, \qquad c_k^{\sigma_r} = -\frac{1}{2}\left(f_{k,1}^{\tau_{r\varphi}} + g_{k,1}^{\sigma_r}\right), \quad d_k^{\sigma_r} = \frac{1}{2}(1-\nu)\,c_k^{\sigma_r}, \\ d_k^{\tau_{r\varphi}} = \frac{1}{2}\left(f_{k,1}^{\tau_{r\varphi}} + d_k^{\sigma_r}\right), \quad (27)$$

$$A_{k,n} = -\frac{1}{n(2n+1)}\left[\frac{1}{2}\,g_{k,2n}^{\tau_{r\varphi}} + n(2n-1)\,B_{k,n}\right], \quad B_{k,n} = \frac{1}{2}\frac{g_{k,2n}^{\tau_{r\varphi}} - f_{k,2n}^{\sigma_r}}{2n-1}, \\ C_{k,n} = \frac{1}{n+1}\left[\frac{f_{k,2n+1}^{\tau_{r\varphi}}}{2(2n+1)} - nD_{k,n}\right], \quad D_{k,n} = -\frac{1}{4n}\left(g_{k,2n+1}^{\sigma_r} + f_{k,2n+1}^{\tau_{r\varphi}}\right). \quad (28)$$

With this all correction stress functions are determined and applying them iteratively will lead to the satisfied addressed boundary conditions. Note that the present calculus does not cover vanishing shear stresses $\tau_{xy}(x,e) = 0$. The negligible effect of this is discussed in the next chapter.

3. Results of the stress analysis

The stress results are discussed and validated using a Finite Element (FE) model built in Abaqus. Its mesh contains CPS8 continuum plane stress elements with 8 nodes. A sinusoidal function in the radial tractions is applied along half of the hole edge to model the bolt contact idealisation. If 72 elements are used therein, convergence in the stresses is reached. The FE model is shown in Fig. 5 together

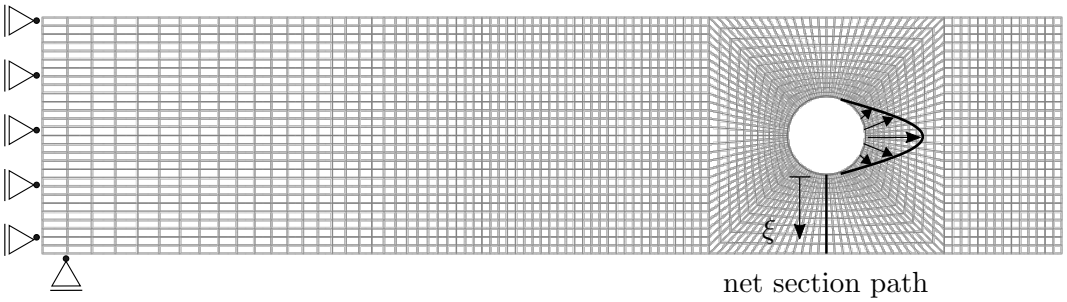

Figure 5. Finite Element model for $w/d = 3,\ e/d = 3$.

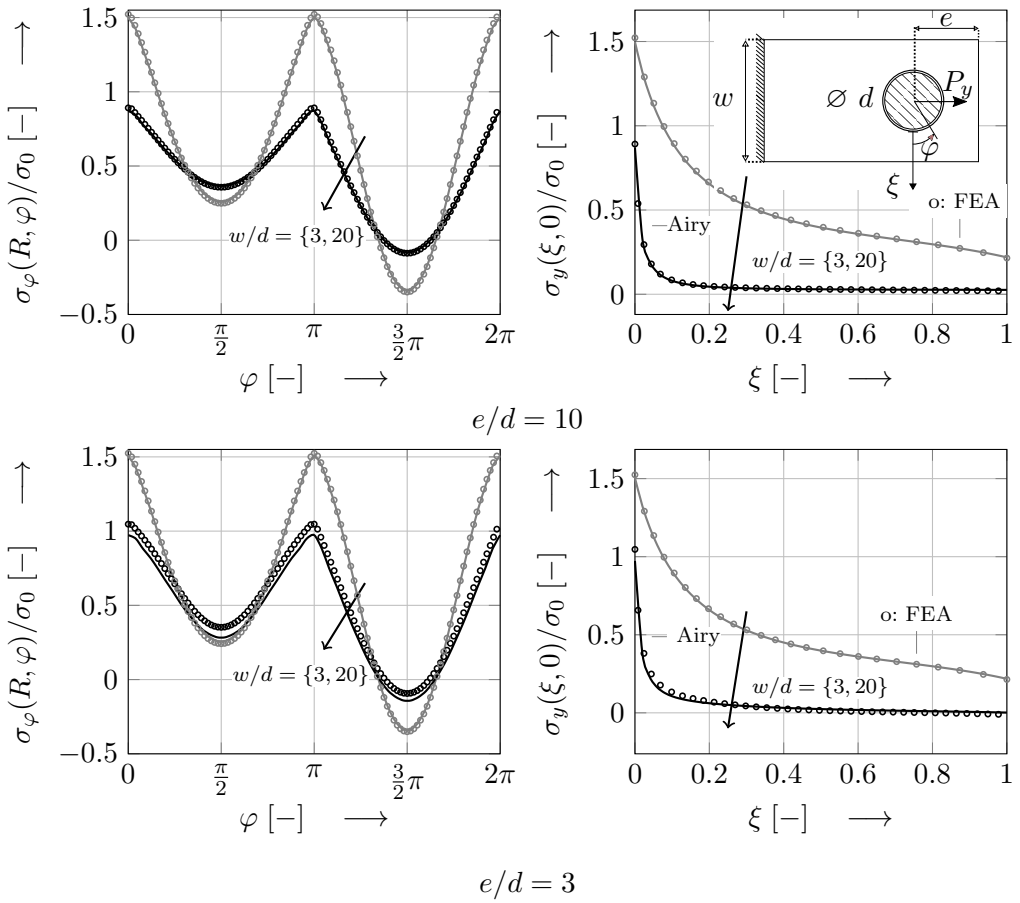

Figure 6. Circumferential and net section stresses. The stresses depend on the Poisson's ratio, for which a value of $\nu = 0.3$ is chosen.

with the dimensionless coordinate

$$\xi = \frac{x - R}{w/2 - R}, \tag{29}$$

where $\xi = 0$ at the hole edge and $\xi = 1$ at the free straight boundary. Let us investigate the characteristic stresses for $w/d = \{3, 20\},\ e/d = \{3, 10\}$ in Fig. 6 and let us take the smallest configuration $w/d = e/d = 3$ with the most pronounced finite dimensions effect for assessment of the present calculus. Excellent results with errors $|\varepsilon| \leq 1$ % within $0 \leq \xi \leq 0.2$ are obtained. This range of the net section

plane has been roughly assumed to be relevant since [35, 37, 38, 50] concerning open holes and [22, 44] regarding bolted joints reveal that in regard of failure analysis by means of nonlocal criteria stress evaluation is needed in the closer hole vicinity. Concerning $w/d = 20, e/d = 3$, errors arise due to nonzero tractions $\tau_{xy}(x, e)$, which cannot be treated by the present calculus. Within $0 \leq \xi \leq 0.2$, $|\varepsilon| \leq 20$ %. However, connections with dimensions $w/d = 20, e/d = 3$ are rather unlikely to be designed since shear-out failure is triggered due to the small relative end distance e/d instead of the fail-safe bearing failure mode. Furthermore, net section failure likely occurs for $w/d \leq 4$ [51] and for those configurations, the stress concentrations mainly arise due to finite width and the end distance e plays an insignificant role. This can be concluded by comparing the characteristic stresses of $e/d = \{3, 10\}$ both with $w/d = 3$. In doing so, a change of the characteristic stresses is hardly noticeable when reducing the relative end distance.

4. Failure analysis

In this section, nonlocal failure criteria in the frameworks of the Theory of Critical Distances (TCD) and Finite Fracture Mechanics (FFM) are briefly introduced. Then, the failure stresses are derived and the hole size effect involving a reduction of the sustainable load with increasing defect size d is modelled. In doing so, the connection width is varied in between $w/d = \{3, 4\}$ with $e/d = 4.17$ enabling to further study the effect of finite dimensions. Moreover, the results of the employed assessment criteria are compared against each other.

4.1. *Theory of Critical Distances*

In the framework of the Theory of Critical Distances (TCD) using line method [35], failure is postulated if the net section stresses averaged along the characteristic distance r_c equal the plain material strength X_T^L. With $x^* = x - R$ as the hole edge distance, this is expressed by

$$\overline{\sigma}_y(r_c) = \frac{1}{r_c} \int_0^{r_c} \sigma_y(x^*, 0)\, \mathrm{d}x^* = X_T^L. \tag{30}$$

The determination of the characteristic distance requires experimentally obtained failure loads. A value of $r_c = 1.143$ mm is derived in [22], which is achieved by taking the experiment NT2 done by [44] and inserting the corresponding failure stress distribution in Eq. (30). The test setting involves a connection with the composite plate material Hexcel IM7-8552 and the quasi-isotropic layup $[90°/0°/\pm 45°]_{3s}$. The hole size effect can be now modelled as follows. For increasing hole diameter d, the relative characteristic distance ξ_{r_c} derived using Eq. (29) decreases and vice versa. Then, with increasing d, the stress evaluation occurs closer to the hole edge involving raised concentrations and the failure criterion is fulfilled for a lower value of σ_{F}. The TCD is hence capable of capturing the physical phenomenon hole size effect. However, the determination of the characteristic distance requires to conduct experiments for calibration. Further, [5, 50, 52–55] have identified the characteristic distance as a structural and not as a material parameter. Hence, it cannot be expected that the value determined based on one bolted joint configuration is ap-

plicable for another but possibly to a certain extent. This matter shall be further investigated by comparing the predictions by the TCD to those predictions by FFM. The latter concept is physically motivated requiring standard material parameters as input data only. Therefore, FFM can be regarded as the more general and sophisticated brittle failure prediction concept. That is why FFM shall serve as reference to assess the capabilities of the TCD.

4.2. *Finite Fracture Mechanics*

In the framework of Finite Fracture Mechanics [42], the instantaneous initiation of a crack with finite length Δa is assumed if both a stress and an energy criterion are satisfied. This condition is referred as coupled criterion established by [40]. In general, determining the minimal load and the corresponding crack length leading to crack initiation is done by solving an optimisation problem. The present bolted joint problem is characterised by a monotonic decrease of the stresses and a monotonic increase of the energy release rate with respect to Δa. With the dimensionless crack length $\Delta\xi = \Delta a/(w/2 - R)$, the coupled criterion specialises to the conditions

$$\begin{aligned} &\frac{1}{\Delta\xi}\int_0^{\Delta\xi} \sigma_y(\xi, 0)\,\mathrm{d}\xi = X_L^T \\ \wedge \quad &\int_0^{\Delta\xi} K_{\mathrm{I}}^2(\xi)\,\mathrm{d}\xi = \int_0^{\Delta\xi} K_{\mathrm{IC}}^2(\xi)\,\mathrm{d}\xi. \end{aligned} \tag{31}$$

Therein, the quantity K_{I} is the mode I stress intensity factor of a newly initiated crack and $K_{\mathrm{IC}}(\xi)$ the R-curve for which a Gompertz function is used. This enables to model a crack length dependence of the fracture toughness $K_{\mathrm{IC}}(\xi)$, which is important if the crack length is of the same order as the process zone l_{pz}. In particular, this occurs for small hole diameters [44]. Regarding the net section stresses, the results of the present calculus are used. Concerning the stress intensity factor K_{I}, data provided in the form of polynomial fitting functions by [44] are inserted. With that a failure analysis can be conveniently reproduced in industry contexts since all field quantities are available in handy form.

4.3. *Discussion*

In Fig. 7, we can observe the FFM calculated crack length Δa reaching a plateau for both finite-width ratios $w/d = \{3, 4\}$. This allows that the crack length may be approximated using a single constant value. Then, the TCD should yield similar predictions as FFM if the characteristic distance lies nearby the plateau. This is true for $r_{c,\mathrm{clb}} = 1.143$ mm, which has been determined based on test data for the geometric ratios $w/d = 1.75,\ e/d = 5.83$. Hence, it can be concluded that the characteristic distance is applicable to configurations with slightly different geometrical properties. This is further confirmed by investigating the failure stresses σ_{F} in Fig. 8. Therein, the predictions by TCD are almost the same as the FFM reference. Relative errors amount $|\varepsilon| \leq 3$ % for $w/d = 3$ and $d \geq 3$ mm as well as $|\varepsilon| \leq 1$ % for $w/d = 4$ and $d \geq 3$ mm. Note that the failure bolt load per plate thickness is $P_{y,\mathrm{F}} = \sigma_{\mathrm{F}} \cdot d$.

Also note that the bearing cut-off is defined as $\sigma_d \approx$700 MPa as in [44]. Above this limit, bearing instead of net section failure is expected to occur. However, setting this limit involves a certain arbitrariness since there exist many definition criteria from which one may freely select. To name a few, these comprise a specific elastic or plastic deformation of the hole or a particular degradation level of the laminate stiffness characterised by a nonlinearity in the load-strain curve. To investigate the finite-width influence on the size effect, let us calculate the failure load reduction factor

$$\eta_d = \frac{\sigma_{\mathrm{F}}(w/d, d)}{\sigma_{\mathrm{F}}(w/d, d = 1\ \mathrm{mm})} \qquad (32)$$

shown in Fig. 9. Therein, a significant reduction involving an asymptotic limit value of about 40 % of the reference failure stress is revealed. The reduction is the more pronounced the wider w/d. The extreme cases of nonlocal failure criteria capable of capturing the hole size effect are $d \to 0$ for which the failure load specialises to the plain material strength and $d \to \infty$ where the predictions coincide with local criteria. The failure stress of a finite-sized hole lies in between and for sufficient material exploitation in lightweight optimal design, the present work emphasizes that nonlocal criteria, which require precisely calculated net section stresses and not only stress concentrations, are crucial.

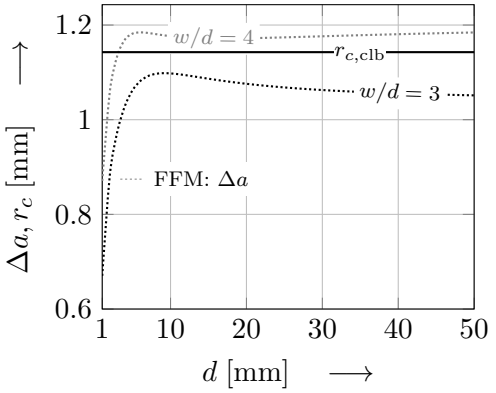

Figure 7. Crack length Δa at failure.

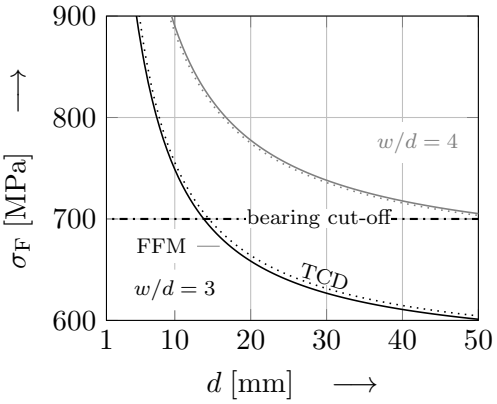

Figure 8. Bearing stresses at failure.

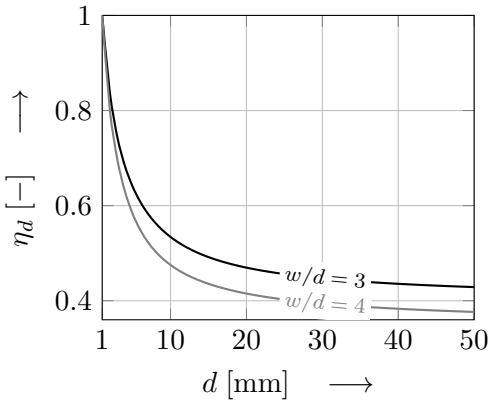

Figure 9. Failure stress reduction

Acknowledgements

Thank you Prof. Jaiani for the invitation and the opportunity to publish in the Lecture Notes of TICMI.

References

[1] P. Camanho, F. Matthews, *Stress analysis and strength prediction of mechanically fastened joints in FRP: a review*, Composites Part A: Applied Science and Manufacturing, **28**, 6 (1997), 529-547

[2] T. Collings, *The strength of bolted joints in multi-directional CFRP laminates*, Composites, **8**, 1 (1977), 43-55

[3] G. Kretsis, F. Matthews, *The strength of bolted joints in glass fibre/epoxy laminates*, Composites, **16**, 2 (1985), 92-102

[4] E. Godwin, F. Matthews, *A review of the strength of joints in fibre-reinforced plastics: Part 1. mechanically fastened joints*, Composites, **11**, 3 (1980), 155- 160

[5] P. Camanho, M. Lambert, *A design methodology for mechanically fastened joints in laminated composite materials*, Composites Science and Technology, **66** (2006) 3004-3020

[6] T. Collings, *On the bearing strengths of CFRP laminates*, Composites, **13**, 3 (1982), 241-252

[7] Y. Xiao, T. Ishikawa, *Bearing strength and failure behavior of bolted composite joints (part i: Experimental investigation)*, Composites Science and Technology, **65**, 7 (2005), 1022-1031

[8] L. J. Hart-Smith, *Mechanically-Fastened Joints for Advanced Composites*, Phenomenological Considerations and Simple Analyses, Springer US, Boston, MA, (1980), 543-574

[9] F. Matthews, *Theoretical stress analysis of mechanically fastened joints*, Elsevier Applied Science Publishers Ltd, Joining Fibre-Reinforced Plastics (1987), 65-103

[10] R. Sevenois, S. Koussios, *Analytic methods for stress analysis of two-dimensional flat anisotropic plates with notches: An overview*, Applied Mechanics Reviews, **66** (2014), 060802

[11] J. P. Waszczak, T. A. Cruse, *Failure mode and strength prediction of anisotropic bolt bearing specimens*, Journal of Composite Materials, **5** (1971), 421-425

[12] W. G. Bickley, *The Distribution of Stress Round a Circular Hole in a Plate*, Philosophical Transactions of the Royal Society of London, **227** (1928), 383-415

[13] R. Knight, *The action of a rivet in a plate of finite breadth*, Philosophy Magazine **19** (Series 7), (1935), 517-540

[14] S. Lekhnitskii, *Anisotropic Plates*, Gordon and Breach Science Publishers, 1968

[15] T. de Jong, *Spanningen rond een gat in een elastisch orthotrope of isotrope plaat, belast door een pen die zich daarin wrijvingsloos kan bewegen*, Technische Hogeschool Delft, Afdeling der Luchtvaart-en Ruimtevaarttechniek, Rapport LR-223.

[16] T. de Jong, *Stresses around pin-loaded holes in elastically orthotropic or isotropic plates*, Journal of Composite Materials, **11** (1977), 313-331.

[17] J. Ogonowski, *Effect of variances and manufacturing tolerances on the design strength and life of mechanically fastened composite joints AFWAL-TR-81-3041, 3*, Technical report, McDonnell Aircraft Company, 1981

[18] C. Echavarra, P. Haller, A. Salenikovich, *Analytical study of a pinloaded hole in elastic orthotropic plates*, Composite Structures, **79**, 1 (2007), 107-112

[19] J. Kratochvil, W. Becker, *Structural analysis of composite bolted joints using the complex potential method*, Composite Structures, **92**, 10 (2010), 2512-2516

[20] B. Grüber, W. Hufenbach, et al., *Stress concentration analysis of fibre-reinforced multilayered composites with pin-loaded holes*, Composites Science and Technology, **67** (2007), 1439-1450

[21] B. Grüber, M. Gude, et al., *Calculation method for the determination of stress concentrations in fibre-reinforced multilayered composites due to metallic interference-fit bolt*, Journal of Composite Materials, **52**, 18 (2018), 2415-2429

[22] M. Nguyen-Hoang, W. Becker, *Tension failure analysis for bolted joints using a closed-form stress solution*, Composite Structures, **238** (2020), 111931

[23] M. Nguyen-Hoang, W. Becker, *Open circular hole in a finite plate under tension treated by airy stress function method*, Springer International Publishing, Cham, (2020), 311-330

[24] M. Nguyen-Hoang, W. Becker, *Stress analysis of finite dimensions bolted joints using the Airy stress function*, in revision, International Journal of Solids and Structures

[25] H. Neuber, *Elastisch-strenge Lösungen zur Kerbwirkung bei Scheiben und Umdrehungskörpern*, ZAMM, **13** (1933), 439-442

[26] H. Neuber, *Zur Theorie der Kerbwirkung bei Biegung und Schub*, Ingenieur-Archiv, **5**, 3 (1934), 238-244

[27] R. Peterson, A. Wahl, *Two and three dimensional cases of stress concentration and comparison with fatigue tests*, Trans. ASME, **58** (1936), A15

[28] H. Neuber, *Kerbspannungslehre: Theorie der Spannungskonzentration, Genaue Berechnung der Festigkeit*, Springer-Verlag, 2013

[29] Z. P. Bažant, I. M. Daniel, Z. Li, *Size Effect and Fracture Characteristics of Composite Laminates*, Journal of Engineering Materials and Technology, **118**, 3 (1996) 317-324

[30] M. Wisnom, *Size effects in the testing of fibre-composite materials*, Composites Science and Technology, **59**, 13 (1999), 1937-1957

[31] G. Dvorak, A. Suvorov, *Size effect in fracture of unidirectional composite plates*, International Journal of Fracture, **95**, 1-4 (1999), 89-101

[32] Z. P. Bažant, *Size effect*, International Journal of Solids and Structures **37**, 1 (2000) 69-80

[33] Z. P. Bažant, Y. Zhou, D. Novák, I. Daniel, *Size effect on flexural strength of fiber-composite laminate*, ASME J. Eng. Mater. Technol, **126**, 1 (2004), 29-37

[34] B. Green, M. Wisnom, S. Hallett, *An experimental investigation into the tensile strength scaling of notched composites*, Composites Part A: Applied Science and Manufacturing, **38**, 3 (2007), 867-878

[35] J. M. Whitney, R. J. Nuismer, *Stress fracture criteria for laminated composites containing stress*

concentrations, Journal of Composite Materials, **8** (1974) 253-265
[36] D. Taylor, *Predicting the fracture strength of ceramic materials using the theory of critical distances*, Engineering Fracture Mechanics, **71**, 16 (2004) 2407-2416
[37] D. Taylor, *The Theory of Critical Distances*, Elsevier Science, 2007
[38] D. Taylor, *The theory of critical distances*, Engineering Fracture Mechanics, **75**, 7 (2008) 1696-1705
[39] D. Taylor, *Applications of the theory of critical distances in failure analysis*, Engineering Failure Analysis, *18*, 2 (2011), 543-549
[40] D. Leguillon, *Strength or toughness? A criterion for crack onset at a notch*, European Journal of Mechanics - A/Solids **21**, 1 (2002), 61-72
[41] P. Cornetti, N. Pugno, A. Carpinteri, D. Taylor, *Finite fracture mechanics: A coupled stress and energy failure criterion*, Engineering Fracture Mechanics **73**, 14 (2006), 2021-2033
[42] P. Weigraeber, D. Leguillon, W. Becker, *A review of finite fracture mechanics: Crack initiation at singular and non-singular stress-raisers*, Archive of Applied Mechanics, **86** (2015), 375-401
[43] J. York, D. Wilson, R. Pipes, *Analysis of the net tension failure mode in composite bolted joints*, Journal of Reinforced Plastics and Composites 1 (2) (1982) 141-152
[44] G. Catalanotti, P. Camanho, *A semi-analytical method to predict net-tension failure of mechanically fastened joints in composite laminates*, Composites Science and Technology, **76** (2013), 69-76
[45] G. Savin, *Stress Concentration Around Holes*, Pergamon Press, 1961
[46] S. Timoshenko, J. N. Goodier, *Theory of Elasticity*, McGraw-Hill Book Company, Inc., 1951.
[47] M. H. Sadd, *Elasticity: Theory, Applications, and Numerics - Second Edition*, Elsevier Butterworth-Heinemann, 2005
[48] J. H. Michell, *On the direct determination of stress in an elastic solid with application to the theory of plates*, Proceedings of the London Mathematical Society, **31** (1899), 100-124
[49] L. N. G. Filon, *On an approximate solution for the bending of a beam of rectangular cross-section under any system of lond, with special reference to points of concentrated or discontinuous loading*, Philosophical Transactions of the Royal Society of London, Series A., **201** (1903), 63-155
[50] P. Camanho, G. Erin, G. Catalanotti, S. Mahdi, P. Linde, *A finite fracture mechanics model for the prediction of the open-hole strength of composite laminates*, Composites Part A: Applied Science and Manufacturing, **43**, 8 (2012) 1219-1225
[51] L. J. Hart-Smith, *Mechanically-fastened joints for advanced composites*, phenomenological considerations and simple analyses, (1980), 543-574
[52] R. B. Pipes, R. C. Wetherhold, J. John W. Gillespie, *Notched strength of composite materials*, Journal of Composite Materials, **13**, 2) (1979), 148-160
[53] J. Awerbuch, M. S. Madhukar, *Notched strength of composite laminates: Predictions and experimentsa review*, Journal of Reinforced Plastics and Composites, **4**, 1 (1985), 3-159
[54] S. C. Tan, *Fracture strength of composite laminates with an elliptical opening*, Composites Science and Technology, **29**, 2 (1987), 133-152
[55] P. Rosendahl, P. Weigraeber, N. Stein, W. Becker, *Asymmetric crack onset at open-holes under tensile and in-plane bending loading*, International Journal of Solids and Structures, **113-114** (2017), 10-23